



Physicochemical studies of aerosols at Montreal Trudeau Airport: The importance of airborne nanoparticles containing metal contaminants[☆]

Mayeesha F. Rahim^a, Devendra Pal^b, Parisa A. Ariya^{a, b, *}

^a Department of Chemistry, McGill University, Montreal, Quebec, Canada

^b Department of Atmospheric and Oceanic Sciences, McGill University, Montreal, Quebec, Canada

ARTICLE INFO

Article history:

Received 3 August 2018

Received in revised form

12 December 2018

Accepted 16 December 2018

Available online 19 December 2018

Keywords:

Nanoparticles

Emerging contaminants

Airport

High particle number density

ABSTRACT

Airborne particles, specifically nanoparticles, are identified health hazards and a key research domain in air pollution and climate change. We performed a systematic airport study to characterize real-time size and number density distribution, chemical composition and morphology of the aerosols (~10 nm–10 μm) using complementary cutting-edge and novel techniques, namely optical aerosol analyzers, triple quad ICP-MS/MS and high-resolution STEM imaging. The total number density of aerosols, predominantly composed of nanoparticles, reached a maximum of $2 \times 10^6 \text{ cm}^{-3}$ and is higher than reported values from any other international airport. We also provide evidence for a wide range of metal in aerosols, and emerging metals in nanoparticles (e.g., Zn and Ni). The geometric mean, median and 99th and 1st percentile values of observed nanoparticle number densities at the apron were 1.0×10^5 , 9.0×10^4 , 1.2×10^6 and $9.3 \times 10^3 \text{ cm}^{-3}$, respectively. These observations were statistically higher than corresponding measurements in downtown Montreal and at major highways during rush hour. This airport is thus a hotspot for nanoparticles containing emerging contaminants. The diurnal trends in concentrations exhibit peaks during flight and rush hours, showing correlations with pollutants such as CO. The HR-TEM-EDS provided evidence for nano-sized particles produced in combustion engines. Implications of our results for air pollution and health are discussed.

© 2018 Elsevier Ltd. All rights reserved.

1. Introduction

Airborne particles, or aerosols, have been shown to have severe implications not only on air pollution, but also on global climate change, as they absorb solar radiation and can alter cloud properties (Forster et al., 2007; Wuebbles et al., 2007). The International Panel on Climate Change stated that “the uncertainty in the global radiation budget from aerosol-cloud interactions is equal to the estimated impact of all anthropogenic green-house gas (GHG) emissions” (Stocker, 2014). This has led the IPCC to conclude that aerosol-cloud interactions “contribute[s] the largest uncertainty to estimates and interpretations of the Earth’s changing energy budget” (Stocker, 2014). Ultrafine particles or airborne

nanoparticles, are a group of aerosols with aerodynamic diameters less than 100 nm. They have also been shown to have severe human health impacts. The health implications of nanotechnology and nanoparticle exposure were thus listed as a key health challenge in 2010 by the World Health Organization (2017).

Airborne nanoparticles originate through photochemical and heterogeneous reactions in the atmosphere, particularly those involving organic compounds or trace metals (Ariya et al., 1999a; Snider et al., 2008; Ariya et al., 2015). Airports have been shown to be sites for anthropogenic airborne nanoparticle emissions that contribute significantly to air pollution in the airport apron and areas surrounding the airport (Kumar et al., 2013). Airport emissions comprise mostly emissions from aircraft engines, the auxiliary power units and ground support equipment, yet some studies have shown that the impact of ground support equipment is much smaller in comparison to aircraft emissions (Unal et al., 2005).

Epidemiological researchers have shown a consistent increase in morbidity and mortality rates in both adults and children with exposure to particulate matter in air (Robert et al., 2004; Delfino

[☆] This paper has been recommended for acceptance by Prof. Wen-Xiong Wang.

* Corresponding author. Postal Address: Department of Chemistry, McGill University, 801 Sherbrooke St. W, Montreal, PQ, H3A 2K6, Canada.

E-mail address: parisa.ariya@mcgill.ca (P.A. Ariya).

et al., 2005; Sarnat et al., 2001). Namely, Dockery et al. demonstrated that chronic exposure to air pollutants is independently related to cardiovascular mortality (Dockery et al., 1993) and Clancy et al. found that decreased air pollution resulted in 116 fewer respiratory deaths and 243 fewer cardiovascular deaths in Dublin per year (Clancy et al., 2002).

The degree of toxicity of nanoparticles is determined by a number of physiochemical properties, such as size distribution, electrostatics, surface area, general morphology and aggregation, which have been shown to affect physiological interactions between particulate matter and target biological areas (Shin et al., 2015). In terms of size, it has been shown that for the deposition of the same amount of particles in the lungs, toxicity tends to increase with decreasing particle size, noting that the total health impact is complex and depends on multiple factors (MacNee and Donaldson, 2003; FERIN et al., 1991). Airborne nanoparticles have been shown to have increased pulmonary toxicity resulting from higher interstitial access along with a large acute inflammatory reaction as determined using lung lavage parameters (Oberdörster et al., 1992).

There are several comprehensive studies on atmospheric aerosols characterization in literature (Traboulsi et al., 2017; Nazarenko et al., 2017a; Rangel-Alvarado et al., 2015; Hu et al., 2016). While many airport measurements of particles are made using filters or impactors and reported measurements are given in mg kg^{-1} of fuel (Masiol and Harrison, 2014; Kinsey et al., 2011; Herndon et al., 2008; Mazaheri et al., 2008; Mazaheri et al., 2011), the number of airborne nanoparticles is a key factor for evaluation of health and climate impacts. To our knowledge, there are only a few studies in literature on the measurement of airborne nanoparticle density in airport ambient air (Mazaheri et al., 2011; Zhu et al., 2011; Ellermann et al., 2012; Hu et al., 2009; Keuken et al., 2015; Hudda and Fruin, 2016). Given the adverse health and climate effects of nanoparticles in ambient air, there are major gaps of knowledge on physical and chemical characteristics and transformation processes of aircraft-generated airborne nanoparticles, which should be further studied (Grassian, 2008; Mudunkotuwa and Grassian, 2011).

During the last few decades, a large number of anthropogenic emerging contaminants have been detected in the environment, mostly in water and soil matrices (Stuart and Compton, 2015). Emerging metal contaminants are generally referred to as synthetic or naturally occurring chemicals, that are not regularly studied in the environment but they have potential to enter the environment and cause adverse ecological and human health effects (Sauvé and Desrosiers, 2014; Sanderson et al., 2014; Hou et al., 2017). They originate from a wide range of human activities including pharmaceutical, construction, cosmetic, medical, pesticidal, industrial, chemical and waste processes. Some of these anthropogenic emerging contaminants are indeed particulate contaminants including nanoplastics and microplastics (Stuart and Compton, 2015). Airborne nanoparticles, including nano-metals, in air, are classified as emerging contaminants (Sýkorová et al., 2017). Several of these emerging metal contaminants also adversely affect human and ecological health by causing ecotoxicity (Hou et al., 2017). Humans are exposed to toxic metals from contaminated air through inhalation, dermal contact and direct or indirect ingestion (Jiang et al., 2017). In contrast to water and soil, not much is known about emerging anthropogenic contaminants in airborne nanoparticles, specifically those related to aerospace activities. Note that as these emerging contaminants are both metal toxicant and health hazard nanoparticles, further research is required to assess their health impacts.

In this study, our objective was to obtain for the first time self-consistent information on the size, abundance and distribution as

well as the chemical composition and morphology of airborne particles between the sizes of a few nm to 10 μm at the apron outside the international terminal and near the Departure Level entrance of the Montreal airport during the summer of 2017. Trudeau Airport is the busiest airport in the province of Quebec, Canada, with annual passenger traffic of 16.6 million. We further investigated the presence of airborne nanoparticles, focusing on metal-containing compounds, in the air surrounding the international airport. Variations in size distribution throughout the day were also analyzed, particularly for rush hours and during precipitation events, in relation to meteorological conditions such as temperature, precipitation and gaseous co-pollutants such as NO_x , ozone and carbon monoxide. We herein discuss the implications of the results on the importance of nanoparticle emissions from an international airport, and future directions of research.

2. Materials and methodology

In this section, we describe the sampling site, *in-situ* measurement of particles and complementary particle sampling for *ex situ* analyses, as well as the suite of optical, mass spectrometry and electron microscopy techniques used in this study. Due to the security restrictions of the airport, we were only allowed several assigned periods of time inside the airport area. As such, we performed comprehensive feasibility experiments during the fall and winter 2016 outside the airport and performed a systematic study of aerosol size distribution, topography and chemical composition, along with time series of various co-pollutants such as O_3 , NO_x ($\text{NO} + \text{NO}_2$), CO, and precipitation from July to September 2017. Real-time *in-situ* aerosol analysis and *ex-situ* aerosol samples were collected at the apron outside the international terminal and near the Departure Level entrance and were compared to samples taken at downtown Montreal at the McGill University downtown campus, which served as a reference. The McGill observatory site is operated in real-time on a daily basis, all year around, with the exception of trouble shooting and field transport. The details of the McGill campus observational site have been explained elsewhere (Dastoor, 2018). Our systematic results are herein presented.

2.1. Sampling site

The particle size distributions were measured *in situ* at the Montréal–Pierre-Elliott-Trudeau International Airport (QC, Canada) by setting up a mobile station at two locations at the airport, the first being on the airport apron outside the international terminal and the second near the airport's Departure Level entrance as shown in Fig. S6 in the Supporting Information. The coordinates of the airport are 45.4697° N, 73.7449° W. Preliminary readings had been taken in December 2016 and the data presented in this paper were taken in a series of pulses in July, August and September 2017.

2.2. Aerosol size distributions

Particle size distributions were measured *in situ* using a NanoScan Scanning Mobility Particle Sizer (SMPS) model 3910 (TSI Inc.) and an Optical Particle Sizer (OPS) model 3330 (TSI Inc.) (TSI, 2010; TSI, 2015). These instruments are factory-calibrated annually with Polystyrene Latex spheres for all internal and external flow rates. The SMPS measures particle size in terms of electric mobility diameter in the range of 10 nm–400 nm while OPS measures the particles in the aerodynamic size range of 0.3–10 μm (optical diameter). The SMPS determines the particles size distribution by deflecting particles by an electric field based on their electric mobility. However, the OPS, measures the optical diameter, which is equivalent to aerodynamic diameter based on a few assumptions

(TSI, 2015). The OPS size distribution was calibrated with Polystyrene Latex (PSL) particles, which are perfectly spherical and have a refractive index of 1.59. When the particles are spherical, the size distribution by the optical counters is equivalent to the actual physical (or geometric) diameter (Chen et al., 2011; Hasheminassab et al., 2014; Hering and McMurry, 1991; Reid et al., 1994). The OPS is strongly dependent on the aerosols characteristics, including the refractive index and dynamic shape factor. Based on the assumption the particles are spherical and particle density is 1 g.cm^{-3} , the optical diameter would be equivalent to aerodynamic diameter and operating the SMPS and OPS simultaneously allows for the measurement of particle sizes from 10 nm to $10 \mu\text{m}$ (Hinds, 1999).

Complementary to *in situ* methods described above, we used a Micro Orifice Uniform Deposit Impactor (MOUDI) to allow size-aggregated collection of particles for further chemical and physical characterization. The impaction stages were greased and a flow rate of 30 L/min was used. The MOUDI was set up for 12-h runs starting at 6 a.m. on three weekdays and a 20-h run starting at 10 a.m., also on a week day. The MOUDI has 8 impaction stages to collect size-fractionated aerosol particle samples. Teflon and Aluminum filters were used as substrates to collect the particles. TEM grids were attached to two stages of the MOUDI, as discussed in the TEM section below. This method is based on a methodology we developed previously and it allows us to perform high resolution transmission electron microscopy directly (Hudson and Ariya, 2007). As such, the collected samples will not be contaminated and their topography after the impact will not be altered.

2.3. High-resolution FEG-TEM and STEM with CCD, EELS and EDS

The TEM-grids were fixed on the filter substrate using double-sided adhesive carbon tape and were placed in the following MOUDI d50 cut-off points: $0.18 \mu\text{m}$ and $1 \mu\text{m}$. Carbon-coated copper grids (SPI supplies, west Chester, PA USA) were chosen to minimize the disturbance of the collected particles and tweezers were used when placing or removing the grids from the substrate to prevent damage (Noël et al., 2013). Several blanks were also taken during the samples. Grids have been placed previously on stages with ultra-pure air as blanks (Hudson and Ariya, 2007).

The field emission gun transmission electron microscope (FEG-TEM) operates with a voltage range of 50–300 kV. The high-brightness, high-coherency gun allows large electron probe currents to be focused onto nanometer-sized areas of the specimen. Capabilities include energy-dispersive X-ray spectroscopy (EDS), electron energy loss spectroscopy (EELS), STEM imaging and mapping and a CCD camera that allows magnification of thin samples (<500 nm) up to >1 million times. The TEM grids were analyzed using a high resolution FEI Tecnai G2F20 S/TEM microscope with a field emission gun, which are relatively new in material sciences and to our knowledge were only used in one of our previous snow particle studies, which is in this study adapted for aerosols (Rangel-Alvarado et al., 2015).

Images were acquired using an Advanced Microscopy Techniques, Corp. (AMT) XR80C CCD Camera System, which we deployed previously for snow particles and, in this study, was adapted for atmospheric aerosols collected directly on the grid, allowing us to study size, morphology and composition (with EDS) of airborne single and aggregated nanoparticles (Rangel-Alvarado et al., 2015). This system allowed us to look at a wide range of aerosol sizes, specifically in the nanoparticle range, with high resolution.

2.4. Total organic carbon (TOC)

To obtain TOC measurements, the substrates were suspended in

40 mL of water and shaken for 24 h. The filter was removed and 2 mL of 10% sodium persulfate was added and combusted at 980°C . A non-dispersive infrared sensor detected the resulting CO_2 gas from these two reactions, separately. A blank was always analyzed using an unused substrate.

2.5. Triple quad inductively coupled plasma mass spectrometry (Triple quad ICP-MS/MS)

To prepare samples for triple quad ICP-MS/MS analysis, the aerosol samples were digested in 2% nitric acid (Omni trace ultra-nitric acid) and ultrapure Milli-Q water in a sealed microwave vessel. The digested aerosol samples were subsequently injected to triple quad ICP-MS to determine trace metal analysis, including: Al, V, Cr, Mn, Fe, Co, Ni, Cu, Zn, As, Se, Sr, Ag, Cd, Ba, Ti, Pb and U. The instrument was optimized using a multi-element calibration standard solution (Agilent Technologies, Standard 2A) containing $10 \mu\text{g/mL}$ of Ag, Al, As, Ba, Be, Ca, Cd, Co, Cr, Cs, Cu, Fe, Ga, K, Li, Mg, Mn, Na, Ni, Pb, Rb, Se, Sr, Tl, U, V and Zn to confirm that interfering species established less than 2% of signal.

3. Results and discussion

In this section, we present our complementary chemical and physical characterization of particles using a suite of cutting-edge techniques, along with complementary co-pollutant and meteorological data (see also the supplementary section) and interpret our results. We also focus on rush hour and precipitation events to further shed light on the role of airport-generated airborne nanoparticles in the biogeochemical cycling of pollutants.

3.1. Evaluation of the abundance and size distribution of particles

The regular time series of size-aggregated particles is shown in Fig. 1 (a). Fig. 1 (b) shows the accumulative *in-situ* airborne aerosol data taken during the study over a 24-h period for the different sized bins measured. Fig. 1 (b) also shows the variations in the number density of particles ranging from 10 nm to $10 \mu\text{m}$ as a function of time. The regular time series of supplementary precipitation rate, temperature, NO_x ($\text{NO} + \text{NO}_2$), O_3 and CO are shown in Fig. 1 (c, d and e).

The total particle number concentration over all sizes at the airport apron (measured on the 20th, 21st and 26th of July) reaches $2.0 \times 10^6 \text{ cm}^{-3}$, which is an order of magnitude higher than the readings taken from near the airport's Departure Level entrance, as illustrated in Fig. 1 (a). Both measurements are significantly higher than the measurements taken in downtown Montreal with heavy traffic, where peak concentrations reach an order of magnitude of 10^4 as measured by researchers in our research group.

The number density of particles at the Montreal Airport apron is also significantly higher than values reported by previous studies at other international airports. Results from a study at a Danish airport showed particle number concentration reached $5 \times 10^5 \text{ per cm}^3$ (Ecocouncil, 2012). Buonanno et al. studied occupational exposure to airborne particles near the runway and hangar of an aviation base and found average concentrations for an 8-h working day to be $2.5 \times 10^4 \text{ particles cm}^{-3}$ and $1.7 \times 10^4 \text{ particles cm}^{-3}$ at the runway and hangar respectively (Buonanno et al., 2012). The only other comparable results were found in a neighborhood adjacent to the regional airport of Santa Monica, where the particle number concentration related to the takeoff phase reached $2.2 \times 10^6 \text{ particles cm}^{-3}$ as reported by Hu et al. (2009). Yet, in this study, we often observe such elevated concentrations for total aerosols, across all size bins, in the ambient air at the airport apron, and not just related to the takeoff phase.

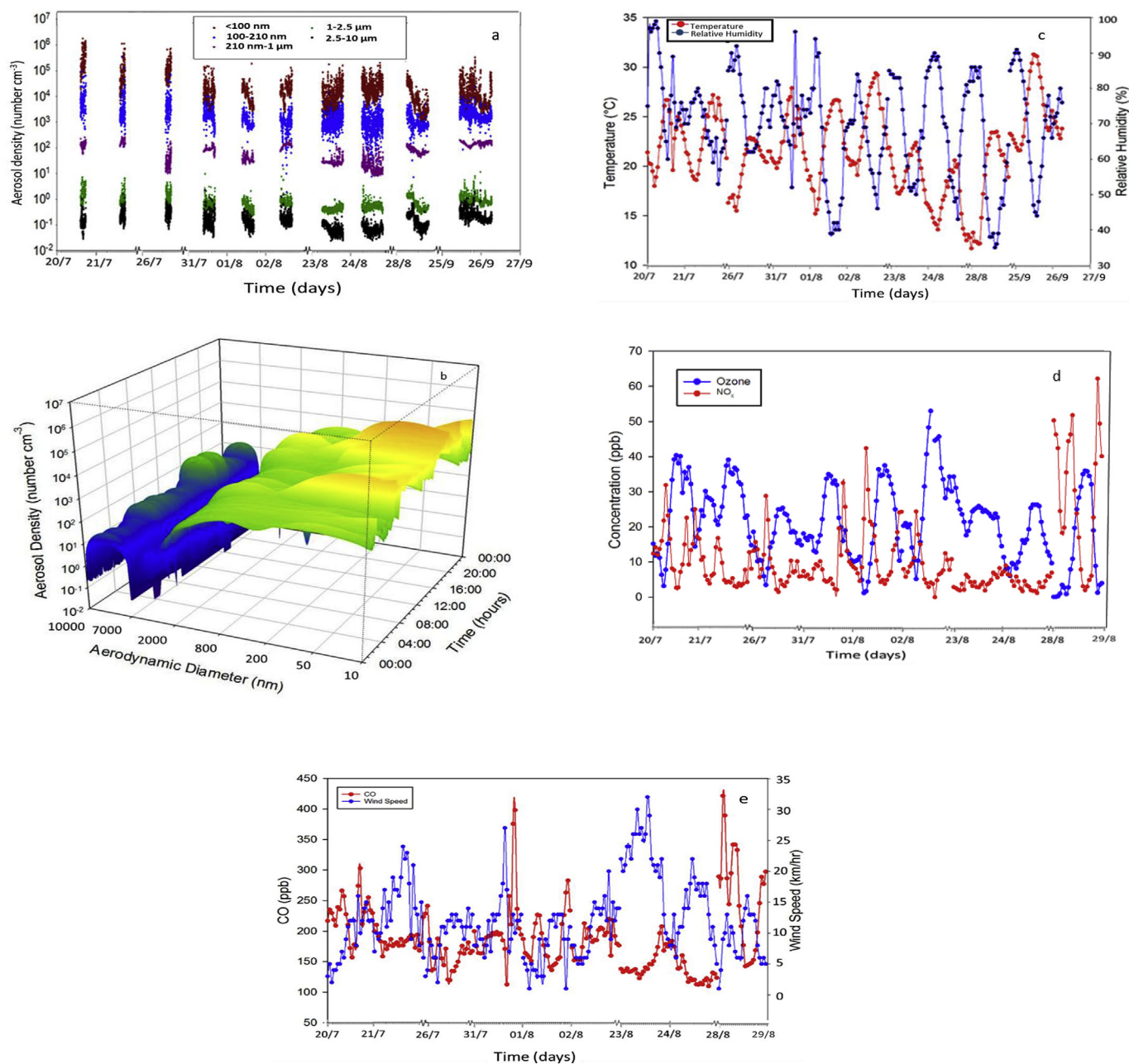


Fig. 1. A schematic depicting (a) the time series of size aggregated particles, (b) accumulated observed real-time data of aerosol number density and size distribution of particles as a function of time, and the time series of supplementary (c) temperature and relative humidity, (d) O₃ and NO_x and (e) CO and wind speed data.

The diurnal variation in the concentration of particles, segregated in terms of location, is shown in Fig. S1 with the combined data shown in Fig. S2 of the Supporting Information. A large fraction of the particles at the airport is smaller than 200 nm and the concentration of particles increases by *c.a.*, 7 orders of magnitude as the particle size decreases from 10 μm to 10 nm. This trend is in accordance with what has been previously observed, that is, the smaller particles are the most abundant particles, in terms of number, in atmosphere (Nazarenko et al., 2017a; Ghoshdastidar et al., 2017).

3.2. Evaluation of the effect of rush hour in the airport on aerosol distribution and density

Illustrated in Fig. 2 (a), we observed relatively lower fluctuations

in the concentrations of airborne nanoparticles before 06:00 and after 24:00. This may be the direct result of lower air traffic between 01:00 and 05:00 as shown in Table S1. The air traffic rush hours coincide with highway rush hours. Between 06:00 to 10:00 and 16:00 to 20:00, while vehicle and airplane traffic reach their peaks, there is a significant jump in airborne nanoparticle concentrations. There are also some fluctuations in nanoparticle concentrations in the mid-afternoon (around 13:00), which is similar to ozone trends and thus likely due to photochemical formation of airborne nanoparticles from its photochemical pathways (Ariya et al., 2000). Note that solar irradiation intensity maximizes around 1 p.m. and several photochemical processes, including those initiated with photolytic oxidants, may lead to the formation of airborne nanoparticles.

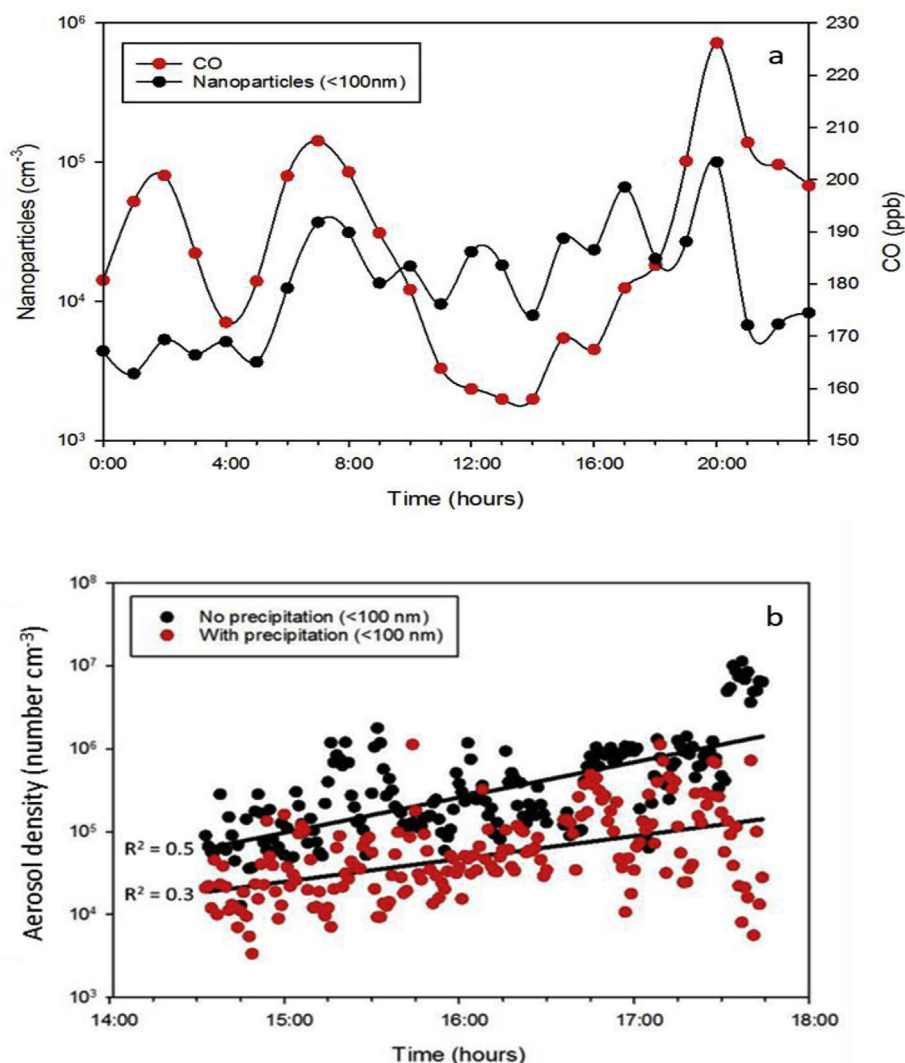


Fig. 2. A schematic depicting (a) the average hourly number density of airborne nanoparticles and concentration of CO and (b) the evaluation of real-time accumulated nanoparticle concentration of size <100 nm during precipitation events depicted in red, in comparison to the absence of any precipitation event, shown in black. All data sets were taken in consecutive days, but similar times have been shown. (For interpretation of the references to colour in this figure legend, the reader is referred to the Web version of this article.)

3.3. Interaction of photochemical and meteorological observations

Air pollution photochemical processes and meteorological factors, such as precipitation, temperature, humidity, wind speed, etc., are closely linked. The hourly temperature and relative humidity data, which were expected to affect particle number densities, are depicted in Fig. 1 (c). The inverse correlation between temperature and relative humidity seen in Fig. 1 (c) is expected (Schneider et al., 2015). While ambient temperature and relative humidity have been shown to impact particle concentrations, the exact dependence of concentrations on temperature and relative humidity is complex and difficult to identify (Wu et al., 2008).

The Spearman correlation coefficient for average hourly ultrafine particle number density and temperature was found to be 0.58 (p value 2×10^{-4}) and for average hourly ultrafine particle number density and relative humidity was found to be -0.39 (p value 2×10^{-4}). The observed positive correlation of ultrafine particle concentration with temperature and negative correlation of ultrafine particle concentration with relative humidity is atypical of results from previous studies on impact of meteorological conditions on particle concentration. Previous studies have found that at

cooler ambient temperatures, the emissions of low and semi volatile compounds favored the formation of new particles as the exhaust mixed with the cooler air (Jamriska et al., 2008; Sabaliauskas et al., 2012) (Jeong et al., 2006). Additionally, already formed particles grow at the lower temperature and corresponding higher level of relative humidity, with increased condensation on these particles (Schneider et al., 2015).

The observed direct relationship between ultrafine particle concentration and temperature can be attributed to meteorological conditions of synoptic scale as observed previously by Schneider et al. (2015). The correlation coefficients for both temperature and relative humidity with ultrafine particle concentration is relatively low. This may be the result of local sources dominating over the effect of meteorological observations through, for example, the emission of primary airborne nanoparticles (Young and Keeler, 2004). It should also be noted that there are counter-acting effects of relative humidity on particle concentrations through different processes such as nucleation, condensation and evaporation which can only be observed in the diurnal particle number concentration variations (Hussein et al., 2006).

In addition to the airborne particles, we also investigated the

link between key gaseous compounds of relevance to urban air pollution, such as ozone, nitrogen oxides, and CO, as shown in Fig. 1 (d and e).

3.4. Anthropogenic source of airborne nanoparticles

The daytime ozone measurement is illustrated in Fig. 1 (d) to demonstrate a photochemical pattern, having a maximum concentration in the early afternoon and minimum concentration during the early morning hours. Such a diurnal pattern is typical for ozone in urban air (Ariya et al., 2000). NO_x continues to act as a catalyst for the photochemical process until it is removed by physical or other chemical processes, thereby resulting in a diurnal pattern opposite to that of ozone, as seen in Fig. 1 (d). The peak in concentration of ozone during the afternoon is the result of the photo-oxidation of a variety of hydrocarbons in the presence of NO_x (Elminir, 2005).

Carbon monoxide is a proxy for anthropogenic emissions in combustion engines (Abdel-Rahman, 1998). Fig. 1 (e) illustrates the diurnal pattern of CO. The concentrations of both CO and airborne nanoparticles peak during rush hours as shown in Fig. 2 (a). The airborne nanoparticle peak coincides with CO concentrations peak, indicating that these gaseous and particulate matter pollutants likely originate from similar sources. The CO emission is predominantly from anthropogenic sources and the level of CO concentration at an airport apron depends on aircraft motions and engine status (Schürmann et al., 2007). As such, we confirm that there is a strong possibility that the observed elevated levels of airborne

nanoparticles arise significantly from anthropogenic emission sources at the airport.

3.5. Emerging nanoparticle contaminants

Besides the number density and distribution of particles, we were interested in understanding their chemical composition. Although we focused on metal analysis, we also performed studies of total organic compounds.

The trace metal concentrations determined through triple ICP-MS/MS analysis are shown in Table 1. In this study, most of the trace metals were observed at nano-size (<180 nm) and submicron size (<320 nm) range. Notwithstanding that several previous studies have reported the trace metal observance in micron size range (Sýkorová et al., 2017; Ahmed et al., 2016; Lee and Von Lehmden, 1973; Celo and Dabek-Zlotorzynska, 2010). Many of these metal or metal oxide nanoparticles are identified in the list of emerging nanoparticle contaminants (Stuart and Compton, 2015), and as confirmed Fig. 3, these metals are in nanoparticles. Out of the metals shown in Table 1, iron (Fe), zinc (Zn), nickel (Ni) and lead (Pb) compounds have been classified as emerging contaminants, while they are in the nanoparticle size range, by the U.S. EPA (EPA and Agency, 2010). Metals that were relatively more abundant in our samples include aluminum (Al), Fe and Zn. Most of the other metals which were detected have also been classified by the U.S. EPA as toxic, including chromium (Cr), manganese (Mn), nickel (Ni), arsenic (As) and lead (Pb).

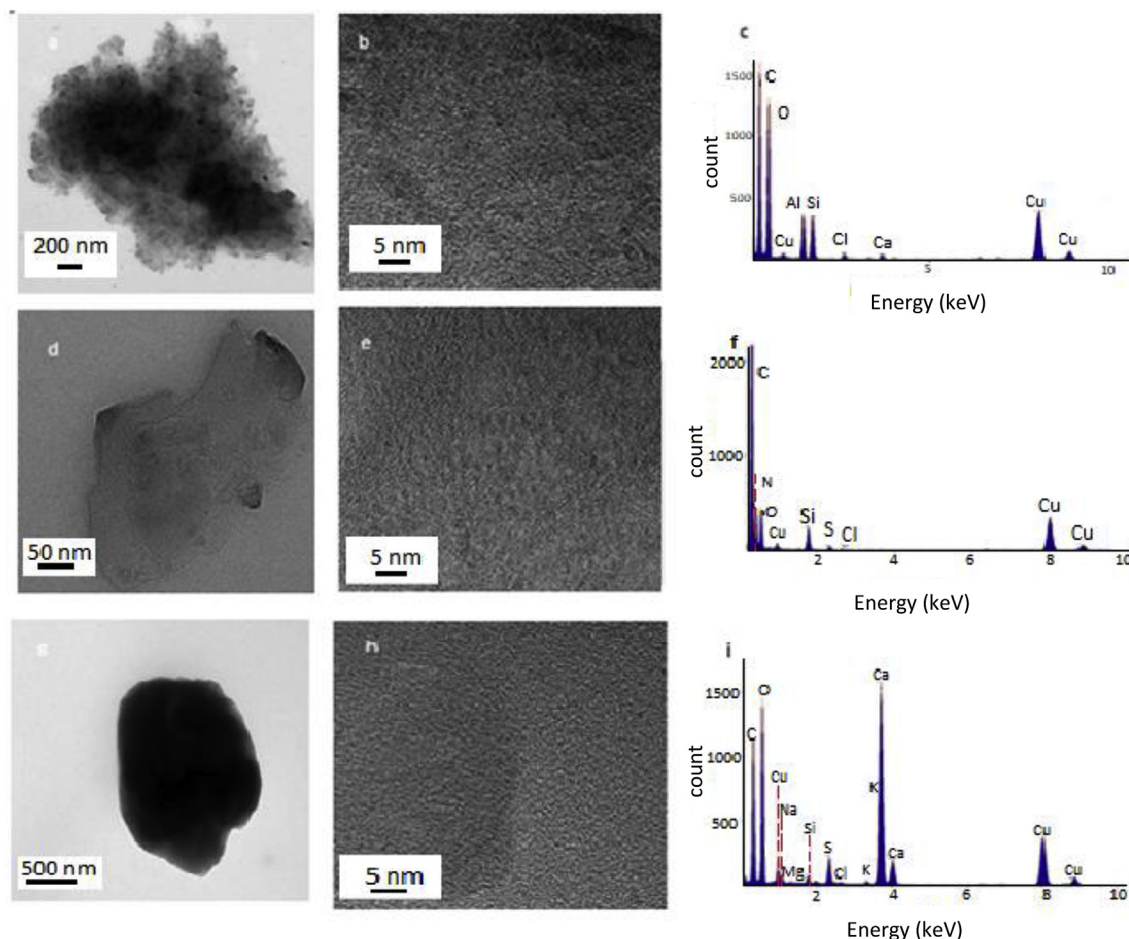


Fig. 3. A typical high resolution transmission electron microscopy (at left hand side) and Energy-dispersive X-ray spectroscopy for both morphology, size and elemental composition of samples taken on grids placed on various stages of a MOUDI impactor. Note our focus was on nano-size particles.

At the airport, elemental iron and zinc comprised the highest masses of all metals detected in this study, as shown in Table 1. Both zinc and iron existed in nano-size particles, including on filters from nano-sized stages of MOUDI (<180 nm and <320 nm). Iron was also observed in micron-size stages of MOUDI. Aluminum maximum concentrations were observed at upper stages of the MOUDI, indicating that these particles are larger than a micron in size. Lead, nickel, chromium and barium were observed mostly in collected filters placed on smaller than one-micron stages.

As shown in Table 1, we measured total organic carbon (TOC) as well. A significant portion of TOC was observed on nano-sized particles, which likely indicates a substantial amount of secondary organic aerosols (SOA), which are formed from anthropogenic as well as natural activities. A major source of SOA formation at the airport is the oxidative processing of aromatic precursors, such as benzene derivatives and phenol emitted from idling aircrafts engines (Kilic et al., 2018).

Table 1 Results of Triple quad ICP-MS/MS and TOC of different concentrations of metals identified in aerosols collected in different size fractions are presented. The size fraction numbers indicate that the collected particles are below the number assigned. For instance, 0.18 μm indicates that the aerosol was collected with diameter less than 180 nm, whereas 0.32 μm indicates particles between 180 nm and 320 nm. The size fraction ranges are based on instrument limitation and interest of research. In the table, ND represents those species that were below detection limit.

$\mu\text{g/L}$	0.18 μm	0.32 μm	0.56 μm	1.0 μm	1.8 μm	3.2 μm	18 μm	LOD
Sr	0.03	0.01	0.00	0.10	0.02	0.04	0.13	0.05
Ba	0.72	0.79	0.79	ND	ND	ND	ND	0.06
Cr	0.28	2.17	0.10	ND	ND	ND	ND	0.04
Mn	0.13	0.22	0.03	ND	ND	0.02	0.12	0.04
Fe	2.49	6.34	−0.19	ND	0.84	3.64	2.58	2.07
Co	0.04	0.02	0.00	ND	0.01	0.00	0.02	0.02
Ni	0.39	2.35	0.11	0.37	ND	−0.05	0.16	0.04
Cu	0.22	0.13	0.03	0.14	0.06	0.10	0.03	0.03
Zn	3.44	0.93	1.06	12.35	ND	ND	1.78	0.15
Cd	0.00	0.00	0.00	0.00	0.00	0.00	0.00	0.02
Ag	0.02	0.01	0.00	0.00	0.00	0.00	0.00	0.02
Mo	0.06	0.05	0.03	0.01	0.03	0.01	0.00	0.03
Al	0.48	0.32	0.43	1.10	1.21	3.09	2.49	0.07
Pb	0.04	0.04	0.02	0.03	0.00	0.00	0.00	0.01
As	0.01	0.01	0.01	ND	ND	0.01	ND	0.02
Sb	0.00	0.01	0.01	0.01	0.00	0.02	0.00	0.03
Se					ND			0.06
TOC		0.5	0.1	0.8	2.0			0.1

3.6. Impact of precipitation on particle distribution: feedback on biogeochemistry?

We have performed air back trajectory analysis for air masses (Rolph et al., 2017; Stein et al., 2015), as shown in Fig. S2 of the Supporting Information. We also found some clear differences in aerosol density due to precipitation as shown in Fig. 2 (b).

The effect of precipitation can be observed by comparing the mass concentration on a day with precipitation to a consecutive day with no precipitation for the same hours at the same location. The results are shown in Fig. 2 (b). We carried out a statistical analysis (*t*-test) for the two sets of data for nanoparticles and found a *p*-value of 9×10^{-8} , indicating that the difference between the populations is significant. Hence, the number density of nanoparticles during the precipitation event has indeed decreased. While this phenomenon may be partially caused by coagulation of particles to form larger-sized particles, there is a net decrease in the total

number of particles, notwithstanding that a level of recovery was observed after the precipitation event.

The consistent observation of metal nanoparticles such Zn, As, Ni, Pb and Cr and their losses during the precipitation events suggest that some portion of nanoparticles, emitted via anthropogenic activities, is removed by precipitation and transferred to the ground surface (soil, water, etc.). Yet, what is the fate of these nanoparticles? Do they enter soil/water/snow/ice matrices and undergo further (photo)chemical or heterogeneous reactions (Ariya et al., 2011)? Or do they undergo transformations and release further aerosols to the atmosphere and add to an already complex atmospheric photochemical reaction pool (Ariya et al., 1999b)? A previous study has shown that heavy metals found in the samples of jet exhaust are present in the sediments of field sites near airports (Boyle, 1996). Lower levels of metals such as copper and beryllium in field sediments compared to in jet exhaust were potentially attributed to chemical transformations and preferential biological uptake of metals in wetland environments. The same study showed a 100% increase in content of copper, beryllium and zinc in sea water and a 50% increase in content of lead after 2 h exposure to jet engine exhaust (Boyle, 1996).

Clearly, the potential secondary reactions are complex and can impact different parts of the ecosystem, particularly close to the airport. There is a large body of studies on the environmental impact of emerging contaminants (Stuart and Compton, 2015). Therefore, we strongly recommend further air pollution, toxicological and biogeochemical studies close to the airport to evaluate the fate of these anthropogenic nanoparticles and their impact on ecosystem and human health.

Previous studies have explicitly shown that snow takes up aerosol and organic pollutants from gasoline engine exhaust and that nanoparticles in snow have efficient ice nucleating properties (Nazarenko et al., 2017a; Rangel-Alvarado et al., 2015; Ariya et al., 1999b). It is also suggested that nanoparticles can affect nucleation processes (Nazarenko et al., 2017a; Kurien et al., 2017). As such, we also recommend future studies on the potential impact of the elevated number density of nanoparticles around the airport on snow contamination and ice nucleation processes.

3.7. Chemical composition and morphology of particles

In addition to Triple quad ICP-MS/MS and total organic compound analysis, shown in Table 1, we used HR-STEM with EDS, which confirmed the existence of emerging contaminants while providing complementary information on size, abundance, topography and chemical composition. The images obtained from HR-TEM analysis are shown in Fig. 3 and indicate an abundance of sub-micron particles. The airborne nanoparticles seem to be non-spherical. Some of them have a high resemblance to soot or “black carbon” particles. Soot particles are aggregates of aciniform morphology composed of individual spherules produced by combustion (Medalia and Rivin, 1982). These compact aggregates are typical to diesel engine emissions and can be expected in samples collected close to ground support vehicles and highway traffic. Black carbon is also a known constituent of aircraft engine emissions (Keuken et al., 2015; Durdina et al., 2017).

Crystal lattices that could be indicative of the presence of four-layered graphene were also seen. A previous study showed that the degree of graphene lamellae ordering of soot particles in aircraft engine particulate matter increases with the thrust level of the aircraft engine (Vander Wal et al., 2014). This can be attributed to an increased temperature at higher thrust levels, which results in the desorption of volatiles as well re-orientation of the carbon chains into more organized structures (Liati et al., 2014; Vander Wal et al., 2007).

While most clusters found in the present study were seen to be bigger than 200 nm, there were also many smaller spheres and rod-like structures that were less than 50 nm in size. The morphology of the clusters were similar to the soot particle clusters containing mainly C found in jet emissions at an airport in Brisbane as reported by Mazaheri et al. (2013).

We observed a significant amount of organic carbon in our substrates, as shown by the results of the TOC, given in Table 1. The TOC values were observed both in nano-size as well as micron-size stages. It is important to note that the particle samples were collected by continuous flow of air through the MOUDI stages over a 20-h period; therefore, a fraction of more volatile organic compound (VOC) particles may have been lost in the sampling process.

As shown in Fig. 3 (c, f and i), the EDS analysis showed several types of airborne nanoparticles with composition similar to emerging metal/metal oxide nano-contaminants. Strong peaks of Cu, Si, and oxygen can be seen and the results are consistent with the ICP-MS/MS observations, presented in Section 3.3. All particles had strong peaks of C, while some particles also showed traces of Al, Cl, Ca, Mg, Na, K, N and S. While jet engines are known to mostly emit primary carbonaceous particles from incomplete combustion, the trace elements can originate from lubrication oil, engine wear, break wear, etc., and S emissions vary with the S content in vehicle and aircraft fuel (Mazaheri et al., 2013; Lesieur and Bonville, 2000; Abegglen et al., 2016; Kazimirova et al., 2016). Other potential sources of trace metals in the atmosphere include AVGAS emissions (Pb), diesel emissions (Al, Ca, Cu, Fe, Mg, Mn, V, Zn), gasoline emissions (Sr, Cu, Mn), non-exhaust traffic sources (Fe, Cu, Sn, Zn), road dust (Zn, Al, K, Fe, Na, Mn), and industrial sources, including metalworking (Fe, K, Na, Pb, Zn), power generation (Ce, Fe, Na, K, V), and furnaces (Cd, Pb, Sb, Zn) (Sanderson et al., 2014; Carr et al., 2011; Daher et al., 2013). Additionally, the ageing of idling aircraft emissions for 3 h has been shown to result in secondary organic aerosols exceeding primary organic aerosols by a factor of 10 (Kilic et al., 2018).

Previous HR-TEM studies on both C and Cu grids and light contrast patterns showed both organic and inorganic carbonaceous compounds in snow samples collected in Montreal (Rangel-Alvarado et al., 2015). Hence, we suspect that the entire carbon evaluated by TOC analysis might not only consist of soot, but also of other organic particles including secondary organic particles, bio-aerosols or bio-organic matter.

3.8. Do the peaks of airborne nanoparticles correspond to airport-related activities?

In this study, we consistently observed that the average and maximum number of particles, observed at the apron, for small particles was higher than outside the entrance door of the airport (Fig. 4). The geometric mean of observed ultrafine particle number densities at the apron and outside the Departure level entrance were $1.0 \times 10^5 \pm 3 \text{ cm}^{-3}$ and $1.1 \times 10^4 \pm 3 \text{ cm}^{-3}$ respectively. The median and 99th and 1st percentile values of observed ultrafine particle number densities at the apron were 9.0×10^4 , 1.2×10^6 and $9.3 \times 10^3 \text{ cm}^{-3}$, respectively. Statistical analysis (*t*-test) of data for airborne nanoparticles observed at the two airport locations gives a *p*-value of 9×10^{-5} indicating the observed nanoparticle density is statistically higher at the apron in comparison with outside the Departure Level entrance.

Complementary to this study, a real-time study of atmospheric particles was concurrently performed in the downtown region of the city of Montreal with readings also taken near a major highway. Even at the peak of heavy traffic jams in the heart of Montreal's anthropogenic activities, the average and maximum number density of aerosols downtown and near the highway were found to be

consistently less than those in the Montreal airport, as shown in Fig. 4.

Note that there is more traffic circulation in the downtown McGill observatory than the Montreal airport. Statistical analysis (*t*-test) of data for airborne nanoparticles observed at the airport apron and downtown location gives a *p*-value of 4×10^{-3} indicating the observed ultrafine particle density at the airport apron is also statistically higher in comparison with downtown readings. The statistically smaller number density of airborne nanoparticles outside the airport entrance in relation to the airport apron and downtown in relation to the airport apron and entrance is a clear indication of the dilution effect. Furthermore, the peak in local airborne nanoparticles at the apron with peak in CO data demonstrates that a significant source of airborne nanoparticles is related to airport activities and not only nearby large traffic.

3.9. Is the montreal airport air quality poor? Or do even clean cities have "hot spots" for aerosol emissions?

As shown in Figs. 2–4 and supplementary materials, indeed values of gaseous air pollutants such as ozone, NO_x, and CO are not at all elevated and are generally lower than cities such as Toronto or Los Angeles. However, the ultrafine particle levels at the apron are more elevated than the measured number density. We wish to emphasize two points. Firstly, we observed that even in the short distance between the apron and the departure terminal entrance, the number density of airborne nanoparticles drastically drops. Yet it was still higher than the downtown measurements during rush hours or any other measurement at major highways around the city. The median levels at the terminal are still comparable to the measured values of cities such as Leicester and several other cities in the world, where the number density was measured (Hama et al., 2017). The second point that should be considered is that there are very limited number density calculations of airborne nanoparticles around the world for airport ambient air, and consequently there are likely several other locations, which will have more elevated concentrations.

We encourage further real-time size aggregated measurements as well as chemical composition of particles including airborne nanoparticles around the world, including potential hot spots such as airports.

4. Future directions: nano-sized emerging contaminant particles and health/environmental effects

It has been known for decades that larger aerosols compose the major mass fraction of all airborne particles, while smaller particles (ultrafine particles) dominate the number density, yet they represent a negligible fraction of the total mass of aerosols. As such, aerosol measurements by weight do not provide valuable insights on the nano-sized particle distribution, which is essential for proper health and air pollution assessments and the improvement of regulations for high emission sources, such as airports.

Forward wind trajectory (Methodology described in Supporting Information & Fig. S3) indicates winds moving in a North Easterly direction through residential areas. As a result of nano-aerosol's small size and slower rates of gravitational settling, nano-sized pollutants may remain suspended in air for longer periods and be more easily transported to greater distances by the wind than larger particles of the same materials (EPA and Agency, 2010).

Due to the increasing evidence for interactions of particles with snow and ice surfaces (Rangel-Alvarado et al., 2015; Mortazavi et al., 2015), including with gas exhaust (Nazarenko et al., 2017a; Nazarenko et al., 2017b; Nazarenko et al., 2016), the role of the interaction with cold ice/snow surfaces should be understood in the

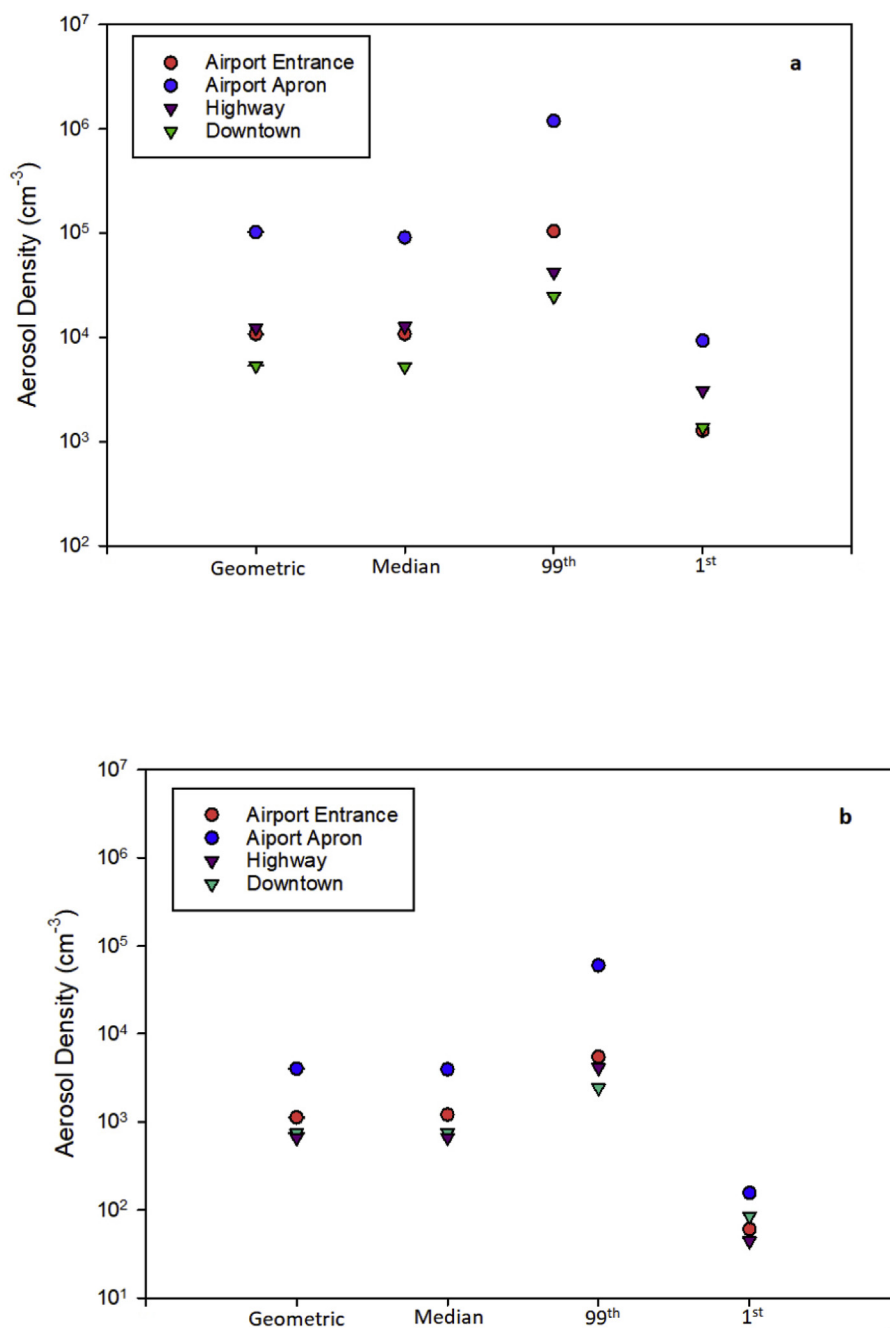


Fig. 4. Comparison of aerosol density measurements of particles with aerodynamic sizes of (a) < 100 nm and (b) 100–200 nm at the airport apron, outside the airport, near a major highway and at the heart of downtown Montreal at McGill University Campus. The geometrical error bars are placed on the data, yet due to their small sizes, they cannot be seen.

airport studies. In a cold-climate city such as Montreal, which receives on average 2.3 m of snow per year due to the existence of a cyclonic updraft and four air masses during fall and winter, conducting further winter studies is advised. Moreover, as precipitation events showed a significant decrease in ultrafine particle abundance in air, further eco-toxicological and biogeochemical studies are needed to evaluate the impact of airport pollutants on human health and urban biogeochemistry.

Despite the observed decrease in the number density from the apron to outside the airport shown in Fig. 4, existing elevated pollution from the airport can potentially affect human and ecosystem health. High levels of airborne nanoparticle exposure are

known to affect human health (Lee et al., 2010). Since many people are working in the airport, and many passengers pass through it, further comprehensive air pollution and health studies are required to evaluate whether the impacts on health are significant. To better understand the fate of the nanoparticles emitted at the airport and their impact on surrounding residential environments, future studies are recommended to measure the aerosol number density in the residential areas downwind of the airport. We also recommend further research and targeted strategies, including recent sustainable technological advances, to reduce the sources of airborne particle emissions related to airport operation and maintenance (e.g., aircraft ground handling, flight procedure, aircraft

fuel system, fueling and leaks, and repair) and human exposure. Some possible strategies include reducing taxi time, use of alternate fuels and gate electrification to reduce ground support equipment and APU use (Policy, 2003).

5. Conclusions

We provided evidence for highly elevated number density of airborne nanoparticles at Montreal airport, which contain different types of emerging contaminants, likely of anthropogenic nature. We also show that the airport is likely a hotspot not only for airborne nanoparticles, but also for emerging contaminants. Back-trajectory analyses indicated that airport pollutants can reach neighbouring populated areas and may cause health concern. As emerging metals are important potential risks to both human and ecosystem health, further studies are recommended to comprehensively understand physical, chemical and biological transformations of emerging metals in airborne nanoparticle form, i.e., the complete life cycle analysis, in the environment. Future studies should focus on concurrent field, laboratory and modeling studies of emerging metal and airborne nanoparticle metals along with their co-pollutants, spatial and temporal variation, their transformation under various environmental conditions including in presence of snow and ice, and their health effects on humans and ecosystems. As emerging metals are important components of air pollution, a complete risk assessment is also recommended.

Acknowledgments

We would like to thank the McGill research chair to PAA, the financial support of the Natural Sciences and Engineering Research Council of Canada including NSERC CRD, and Environment and Climate Change Canada, and collaborations with the City of Montreal, ETS, and Aerospatiale Consortium in Quebec. Especially, we would like to particularly thank Lyne Michaud (Aéroports de Montréal, Canada) for the provision of sampling sites, and excellent sampling accommodation, which allowed our students to perform sampling in a safe and systematic manner. Dominic Bélanger and Marc Amyot (Université de Montréal, Canada) for help with the ICP MS technique, David Liu (McGill University, Canada) for the TEM technique and Katherine Velghe (Université du Québec à Montréal, Canada) for the TOC technique. We also thank Emma Morris and Jessica Di Bartolomeo for their help in proofreading the manuscript.

Appendix A. Supplementary data

Supplementary data to this article can be found online at <https://doi.org/10.1016/j.envpol.2018.12.050>.

References

- Abdel-Rahman, A., 1998. On the emissions from internal-combustion engines: a review. *Int. J. Energy Res.* 22 (6), 483–513.
- Abegglen, M., et al., 2016. Chemical characterization of freshly emitted particulate matter from aircraft exhaust using single particle mass spectrometry. *Atmos. Environ.* 134, 181–197.
- Ahmed, M., Guo, X., Zhao, X.-M., 2016. Determination and analysis of trace metals and surfactant in air particulate matter during biomass burning haze episode in Malaysia. *Atmos. Environ.* 141, 219–229.
- Ariya, P.A., et al., 1999. Polar sunrise experiment 1995: hydrocarbon measurements and tropospheric Cl and Br-atoms chemistry. *Atmos. Environ.* 33 (6), 931–938.
- Ariya, P.A., Hopper, J.F., Harris, G.W., 1999. C2-C7 hydrocarbon concentrations in Arctic snowpack interstitial air: potential presence of active Br within the snowpack. *J. Atmos. Chem.* 34 (1), 55–64.
- Ariya, P.A., Sander, R., Crutzen, P.J., 2000. Significance of HO_x and peroxides production due to alkene ozonolysis during fall and winter: a modeling study. *J. Geophys. Res.: Atmosphere* 105 (D14), 17721–17738.
- Ariya, P., et al., 2011. Snow—a photobiological exchange platform for volatile and semi-volatile organic compounds with the atmosphere. *Environ. Chem.* 8 (1), 62–73.
- Ariya, P.A., et al., 2015. Mercury physicochemical and biogeochemical transformation in the atmosphere and at atmospheric interfaces: a review and future directions. *Chem. Rev.* 115 (10), 3760–3802.
- Boyle, K., 1996. Evaluating particulate emissions from jet engines: analysis of chemical and physical characteristics and potential impacts on coastal environments and human health. *Transport. Res. Rec.: Journal of the Transportation Research Board* (1517), 1–9.
- Buonanno, G., et al., 2012. Occupational exposure to airborne particles and other pollutants in an aviation base. *Environ. Pollut.* 170, 78–87.
- Carr, E., et al., 2011. Development and evaluation of an air quality modeling approach to assess near-field impacts of lead emissions from piston-engine aircraft operating on leaded aviation gasoline. *Atmos. Environ.* 45 (32), 5795–5804.
- Celo, V., Dabek-Zlotorzynska, E., 2010. Concentration and source origin of trace metals in PM_{2.5} collected at selected Canadian sites within the Canadian national air pollution surveillance program. In: *Urban Airborne Particulate Matter*. Springer, pp. 19–38.
- Chen, G., et al., 2011. Observations of Saharan dust microphysical and optical properties from the Eastern Atlantic during NAMMA airborne field campaign. *Atmos. Chem. Phys.* 11 (2), 723–740.
- Clancy, L., et al., 2002. Effect of air-pollution control on death rates in Dublin, Ireland: an intervention study. *Lancet* 360 (9341), 1210–1214.
- Daher, N., et al., 2013. Seasonal and spatial variability in chemical composition and mass closure of ambient ultrafine particles in the megacity of Los Angeles. *Environ. Sci. J. Integr. Environ. Res.: Processes & Impacts* 15 (1), 283–295.
- Dastoor, D.P.P.A.A.A., 2018. Physical and chemical measurement of aerosols in montreal: the existence of airborne nano-sized emerging contaminants. *J. Geophys. Res.* submitted for publication.
- Delfino, R.J., Sioutas, Constantinos, Malik, Shaista, 2005. Potential role of ultrafine particles in associations between airborne particle mass and cardiovascular health. *Environ. Health Perspect.* 113 (8), 946.
- Dockery, D.W., et al., 1993. An association between air pollution and mortality in six US cities. *N. Engl. J. Med.* 329 (24), 1753–1759.
- Durdina, L., et al., 2017. Assessment of particle pollution from jetliners: from smoke visibility to nanoparticle counting. *Environ. Sci. Technol.* 51 (6), 3534–3541.
- Ecocouncil, D., 2012. Air Pollution in Airports Ultrafine Particles, Solutions and Successful Cooperation.
- Ellermann, T., et al., 2012. Assessment of the Air Quality at the Apron of Copenhagen Airport Kastrup in Relation to the Occupational Environment.
- Elminir, H.K., 2005. Dependence of urban air pollutants on meteorology. *Sci. Total Environ.* 350 (1), 225–237.
- EPA, U., 2010. In: Agency, E.P. (Ed.), *Emerging Contaminants – Nanomaterials*.
- FERIN, J., et al., 1991. Pulmonary tissue access of ultrafine particles. *J. Aerosol Med.* 4 (1), 57–68.
- Forster, P., et al., 2007. Changes in atmospheric constituents and in radiative forcing (Chapter 2), in *Climate Change 2007 The Physical Science Basis* 139–234. <https://globalchange.mit.edu/publication/13723>.
- Ghoshdastidar, A.J., et al., 2017. Exposure to Nanoscale and Microscale Particulate Air Pollution Prior to Mining Development Near a Northern Indigenous Community in Québec, Canada. *Environmental Science & Pollution Research*.
- Grassian, V.H., 2008. When size really matters: size-dependent properties and surface chemistry of metal and metal oxide nanoparticles in gas and liquid phase environments. *J. Phys. Chem. C* 112 (47), 18303–18313.
- Hama, S.M., et al., 2017. Sub-micron particle number size distribution characteristics at two urban locations in Leicester. *Atmos. Res.* 194, 1–16.
- Hasheminassab, S., et al., 2014. Diurnal and seasonal trends in the apparent density of ambient fine and coarse particles in Los Angeles. *Environ. Pollut.* 187, 1–9.
- Hering, S.V., McMurry, P.H., 1991. Optical counter response to monodisperse atmospheric aerosols. *Atmos. Environ. Part A. General Topics* 25 (2), 463–468.
- Herndon, S.C., et al., 2008. Commercial aircraft engine emissions characterization of in-use aircraft at Hartsfield-Jackson Atlanta International Airport. *Environ. Sci. Technol.* 42 (6), 1877–1883.
- Hinds, W.C., 1999. *Aerosol Technology: Properties, Behavior, and Measurement of Airborne Particles*, 2nd.
- Hou, D., et al., 2017. Integrated GIS and multivariate statistical analysis for regional scale assessment of heavy metal soil contamination: a critical review. *Environ. Pollut.* 1188–1200.
- Hu, S., et al., 2009. Aircraft emission impacts in a neighborhood adjacent to a general aviation airport in Southern California. *Environ. Sci. Technol.* 43 (21), 8039–8045.
- Hu, Z., et al., 2016. Development of a green technology for mercury recycling from spent compact fluorescent lamps using iron oxides nanoparticles and electrochemistry. *ACS Sustain. Chem. Eng.* 4 (4), 2150–2157.
- Hudda, N., Fruin, S., 2016. International airport impacts to air quality: size and related properties of large increases in ultrafine particle number concentrations. *Environ. Sci. Technol.* 50 (7), 3362–3370.
- Hudson, E.D., Ariya, P.A., 2007. Measurements of non-methane hydrocarbons, DOC in surface ocean waters and aerosols over the Nordic seas during polarstern cruise ARK-XX/1 (2004). *Chemosphere* 69 (9), 1474–1484.
- Hussein, T., et al., 2006. Meteorological dependence of size-fractionated number concentrations of urban aerosol particles. *Atmos. Environ.* 40 (8), 1427–1440.
- Jamriska, M., Morawska, L., Mergersen, K., 2008. The effect of temperature and humidity on size segregated traffic exhaust particle emissions. *Atmos. Environ.* 42 (10), 2369–2382.

- Jeong, C.-H., et al., 2006. Influence of atmospheric dispersion and new particle formation events on ambient particle number concentration in Rochester, United States, and Toronto, Canada. *J. Air Waste Manag. Assoc.* 56 (4), 431–443.
- Jiang, Y., et al., 2017. Source apportionment and health risk assessment of heavy metals in soil for a township in Jiangsu Province, China. *Chemosphere* 168, 1658–1668.
- Kazimirova, A., et al., 2016. Automotive airborne brake wear debris nanoparticles and cytokinesis-block micronucleus assay in peripheral blood lymphocytes: a pilot study. *Environ. Res.* 148, 443–449.
- Keuken, M., et al., 2015. Total and size-resolved particle number and black carbon concentrations in urban areas near Schiphol airport (The Netherlands). *Atmos. Environ.* 104, 132–142.
- Kilic, D., et al., 2018. Identification of secondary aerosol precursors emitted by an aircraft turbofan. *Atmos. Chem. Phys.* 18 (10), 7379–7391.
- Kinsey, J., et al., 2011. Chemical characterization of the fine particle emissions from commercial aircraft engines during the aircraft particle emissions experiment (APEX) 1 to 3. *Environ. Sci. Technol.* 45 (8), 3415–3421.
- Kumar, P., et al., 2013. Nanoparticle emissions from 11 non-vehicle exhaust sources—A review. *Atmos. Environ.* 67, 252–277.
- Kurien, U., et al., 2017. Radiation enhanced uptake of Hg 0 (g) on iron (oxyhydr) oxide nanoparticles. *RSC Adv.* 7 (71), 45010–45021.
- Lee Jr., R.E., Von Lehmden, D.J., 1973. Trace metal pollution in the environment. *J. Air Pollut. Contr. Assoc.* 23 (10), 853–857.
- Lee, J.H., et al., 2010. Challenges and perspectives of nanoparticle exposure assessment. *Toxicological research* 26 (2), 95.
- Lesieur, R.R. and L.J. Bonville Jr, System and Method for Desulfurizing Gasoline or Diesel Fuel to Produce a Low Sulfur-content Fuel for Use in an Internal Combustion Engine. 2000, Google Patents.
- Liat, A., et al., 2014. Electron microscopic study of soot particulate matter emissions from aircraft turbine engines. *Environ. Sci. Technol.* 48 (18), 10975–10983.
- MacNee, W., Donaldson, K., 2003. Mechanism of lung injury caused by PM10 and ultrafine particles with special reference to COPD. *Eur. Respir. J.* 21 (40 Suppl. 1), 47s–51s.
- Masiol, M., Harrison, R.M., 2014. Aircraft engine exhaust emissions and other airport-related contributions to ambient air pollution: a review. *Atmos. Environ.* 95, 409–455.
- Mazaheri, M., Johnson, G.R., Morawska, L., 2008. Particle and gaseous emissions from commercial aircraft at each stage of the landing and takeoff cycle. *Environ. Sci. Technol.* 43 (2), 441–446.
- Mazaheri, M., Johnson, G., Morawska, L., 2011. An inventory of particle and gaseous emissions from large aircraft thrust engine operations at an airport. *Atmos. Environ.* 45 (20), 3500–3507.
- Mazaheri, M., et al., 2013. Composition and morphology of particle emissions from in-use aircraft during takeoff and landing. *Environ. Sci. Technol.* 47 (10), 5235–5242.
- Medalia, A.I., Rivin, D., 1982. Particulate carbon and other components of soot and carbon black. *Carbon* 20 (6), 481–492.
- Mortazavi, R., Attiya, S., Ariya, P., 2015. Arctic microbial and next-generation sequencing approach for bacteria in snow and frost flowers: selected identification, abundance and freezing nucleation. *Atmos. Chem. Phys.* 15 (11), 6183–6204.
- Mudunkotuwa, I.A., Grassian, V.H., 2011. The devil is in the details (or the surface): impact of surface structure and surface energetics on understanding the behavior of nanomaterials in the environment. *J. Environ. Monit.* 13 (5), 1135–1144.
- Nazarenko, Y., et al., 2016. Role of snow and cold environment in the fate and effects of nanoparticles and select organic pollutants from gasoline engine exhaust. *Environ. Sci. J. Integr. Environ. Res.: Processes & Impacts* 18 (2), 190–199.
- Nazarenko, Y., et al., 2017. Role of snow in the fate of gaseous and particulate exhaust pollutants from gasoline-powered vehicles. *Environ. Pollut.* 223, 665–675.
- Nazarenko, Y., et al., 2017. Novel aerosol analysis approach for characterization of nanoparticulate matter in snow. *Environ. Sci. Pollut. Control Ser.* 24 (5), 4480–4493.
- Noël, A., et al., 2013. Assessment of the contribution of electron microscopy to nanoparticle characterization sampled with two cascade impactors. *J. Occup. Environ. Hyg.* 10 (3), 155–172.
- Oberdörster, G., et al., 1992. Role of the alveolar macrophage in lung injury: studies with ultrafine particles. *Environ. Health Perspect.* 97, 193.
- Organization, W.H., 2017. Parma Declaration on Environment and Health, Fifth Ministerial Conference on Environment and Health “Protecting Children’s Health in a Changing Environment”.
- Policy, N.S.f.C.A.U.M.C.f.C.A., 2003. Controlling Airport-related Air Pollution.
- Rangel-Alvarado, R.B., Nazarenko, Y., Ariya, P.A., 2015. Snow-borne nanosized particles: abundance, distribution, composition, and significance in ice nucleation processes. *J. Geophys. Res.: Atmos.* 120 (22).
- Reid, J.S., et al., 1994. Geometric/aerodynamic equivalent diameter ratios of ash aggregate aerosols collected in burning Kuwaiti well fields. *Atmos. Environ.* 28 (13), 2227–2234.
- Robert, D., Brook, M.B.F., Wayne, Cascio, Hong, Yuling, George Howard, P.M.L., Russell, Luepker, Murray, Mittleman, Jonathan Samet Jr., M.S.C.S., Ira, Tager, 2004. Air Pollution and Cardiovascular Disease: a Statement for Healthcare Professionals from the Expert Panel on Population and Prevention Science of the American Heart Association. American Heart Association.
- Rolph, G., Stein, A., Stunder, B., 2017. Real-time environmental applications and display system: Ready. *Environ. Model. Software* 95, 210–228.
- Sabalaiuskas, K., et al., 2012. Five-year roadside measurements of ultrafine particles in a major Canadian city. *Atmos. Environ.* 49, 245–256.
- Sanderson, P., Delgado-Saborit, J.M., Harrison, R.M., 2014. A review of chemical and physical characterisation of atmospheric metallic nanoparticles. *Atmos. Environ.* 94, 353–365.
- Sarnat, J.A., Schwartz, Joel, Suh, Helen H., 2001. Fine particulate air pollution and mortality in 20 US cities. *N. Engl. J. Med.* 344 (16), 1253–1254.
- Sauvé, S., Desrosiers, M., 2014. A review of what is an emerging contaminant. *Chem. Cent. J.* 8 (1), 15.
- Schneider, I.L., et al., 2015. Atmospheric particle number concentration and size distribution in a traffic-impacted area. *Atmos. Pollut. Res.* 6 (5), 877–885.
- Schürmann, G., et al., 2007. The impact of NOx, CO and VOC emissions on the air quality of Zurich airport. *Atmos. Environ.* 41 (1), 103–118.
- Shin, S.W., Song, I.H., Um, S.H., 2015. Role of physicochemical properties in nanoparticle toxicity. *Nanomaterials* 5 (3), 1351–1365.
- Snider, G., Raofie, F., Ariya, P.A., 2008. Effects of relative humidity and CO (g) on the O 3-initiated oxidation reaction of Hg 0 (g): kinetic & product studies. *Phys. Chem. Chem. Phys.* 10 (36), 5616–5623.
- Stein, A., et al., 2015. NOAA’s HYSPLIT atmospheric transport and dispersion modeling system. *Bull. Am. Meteorol. Soc.* 96 (12), 2059–2077.
- Stocker, T., 2014. Climate Change 2013: the Physical Science Basis: Working Group I Contribution to the Fifth Assessment Report of the Intergovernmental Panel on Climate Change. Cambridge University Press.
- Stuart, E.J., Compton, R.G., 2015. Nanoparticles-emerging contaminants. In: *Environmental Analysis by Electrochemical Sensors and Biosensors*. Springer, pp. 855–878.
- Sýkorová, B., et al., 2017. Heavy metals in air nanoparticles in affected industry area. *J. Sustain. Dev. Energy, Water Environ. Syst.* 5 (1), 58–68.
- Traboulsi, H., et al., 2017. Inhaled pollutants: the molecular scene behind respiratory and systemic diseases associated with ultrafine particulate matter. *Int. J. Mol. Sci.* 18 (2), 243.
- TSI, 2010. Aerosol Instrument Manager® Software for Scanning Mobility Particle Sizer™ (SMPS™) Spectrometer User’s Manual.
- TSI, 2015. Multi-instrument Manager (MIM™) Software—building Particle Size Distributions from SMPS™, Nanoscan SMPS, and OPS Data.
- Unal, A., et al., 2005. Airport related emissions and impacts on air quality: application to the Atlanta International Airport. *Atmos. Environ.* 39 (32), 5787–5798.
- Vander Wal, R.L., et al., 2007. HRTEM Study of diesel soot collected from diesel particulate filters. *Carbon* 45 (1), 70–77.
- Vander Wal, R.L., Bryg, V.M., Huang, C.-H., 2014. Aircraft engine particulate matter: macro-micro- and nanostructure by HRTEM and chemistry by XPS. *Combust. Flame* 161 (2), 602–611.
- Wu, Z., et al., 2008. Particle number size distribution in the urban atmosphere of Beijing, China. *Atmos. Environ.* 42 (34), 7967–7980.
- Wuebbles, D., Gupta, M., Ko, M., 2007. Evaluating the impacts of aviation on climate change. *Eos, Trans. Am. Geophys. Union* 88 (14), 157–160.
- Young, L.-H., Keeler, G.J., 2004. Characterization of ultrafine particle number concentration and size distribution during a summer campaign in southwest Detroit. *J. Air Waste Manag. Assoc.* 54 (9), 1079–1090.
- Zhu, Y., et al., 2011. Aircraft emissions and local air quality impacts from takeoff activities at a large International Airport. *Atmos. Environ.* 45 (36), 6526–6533.